Supporting Information: Reactivity among first and second coordination spheres using a multiprotonated ligand and Cu(II) in the solid-state.

Haitao Li[a], Yuxia Yang[a], Antonino Famulari[b], Lianxin Xin[a], Javier Martí-Rujas,[b,c] Fang Guo*[a]*

[a]College of Chemistry, Liaoning University, Shenyang 110036, China.

[b]Dipartimento di Chimica Materiali e Ingegneria Chimica. ‘‘Giulio Natta’’, Politecnico di Milano, Via L. Mancinelli 7, 20131 Milan, Italy.

[c]Center for Nano Science and Technology@Polimi, Istituto Italiano di Tecnologia, Via Pascoli 70/3, 20133 Milano, Italy.

Contents

Dehydrochlorination reaction (3→4). Synthesis of [$LCuCl_2$] (4)

Chemisorption of HCl and H_2O Vapours. First-to-second coordination sphere reaction 4→3.

Flux synthesis of complex 4

Low-Pressure Nitrogen Adsorption/Desorption Measurements

Figure S1. Images of the single crystals of compounds **1**, **2**, **3**, and **4**.

Figure S2. Packing of **1** viewed along the *a*-axis. Color code: carbon: orange; nitrogen: blue; oxygen: red; chloride: green; hydrogen: white.

Figure S3. Packing of **2** viewed along the *c*-axis. Color code: carbon: orange; nitrogen: blue; chloride: green; copper: brown; hydrogen: white.

Figure S4. Packing of **3** viewed along the *a*-axis. Color code: carbon: orange; nitrogen: blue; oxygen**:** red**;** chloride: green; copper: brown; hydrogen: white.

Figure S5. Coordination geometries around the $[CuCl_4]^{2-}$ metal center in **2** (a). The disordered atoms in the $[CuCl_4]^{2-}$ have not been shown for clarity purposes. View of the $[CuCl_3(H_2O)]^-$ in **3**: top (b) and side views (c).

Figure S6. Crystal structure of **4** showing the hydrogen bond and short contacts along the *a*-axis. Color code: carbon: orange; nitrogen: blue; oxygen**:** red**;** chloride: green; copper: brown; hydrogen: white.

Figure S7. Packing of **4** viewed along the *a*-axis. Color code: carbon: orange; nitrogen: blue; oxygen**:** red**;** chloride: green; copper: brown; hydrogen: white.

Table S1. Hydrogen bonds in crystal **2**.

Table S2. Hydrogen bonds in crystal **3**.

Table S3. Hydrogen bond and short interactions in crystal **4**.

Figure S8. TGA corresponding to second sphere adducts **2** and **3**.

Figure S9. DSC corresponding to second sphere adduct **3**.

Figure S10. DSC corresponding to the coordination complex **4**.

Figure S11. Nitrogen adsorption/desorption isotherms of the powder of **3** (a) and **4** (b).

Figure S12. (a) Simulated XRPD from single crystal **1**. (b) The product of grinding salt of **L** and $CuCl_2 \cdot 2H_2O$ in 1:1 ratio with a drop of concentrated HCl and a drop of methanol for 5 minutes. (c) Simulated XRPD from single crystal **3**.

Figure S13. Experimental XRPD patterns of **1**: (a) Simulated XRPD from single crystal **1**; (b) Experimental XRPD from single crystal **1**.

Figure S14. Experimental XRPD patterns of crystal **2**: (a) Simulated XRPD from single crystal **2**; (b) Experimental XRPD from single crystal **2**.

Figure S15. Experimental XRPD patterns of crystal **3**: (a) Simulated XRPD from single crystal **3**; (b) Experimental XRPD from single crystal **3**.

Figure S16. Experimental XRPD patterns of crystal **4**: (a) Simulated XRPD from single crystal **4**; (b) Experimental XRPD from single crystal **4**.

Table S5. Crystal data and structural refinement parameters for **1–4**.

Table S6 DFT energies relating to the reaction $[CuCl_4]^{2-} + H_2O \rightarrow [CuCl_3H_2O]^- + Cl^-$. Total energies are reported in hartree while differences both in hartree and kcal/mol.

Table S7 Solid state DFT energies relating to crystalline structures **2** and **3**. Total energies are reported in hartree while differences both in hartree and kcal/mol.

Molecular Modelling Data

Materials and Methods

All chemicals were obtained from commercial sources and used without further purification. Powder X-ray diffraction measurements were performed with a Bruker D8 diffractometer (λ = 1.54056 Å). TGA data were obtained using a TGA/SDTA851e thermogravimetric analyzer with a scan rate of 10°C min^{-1}. DSC experiments were performed using METTLER DSC1/700 at a heating rate of 10 °C min^{-1} in a stream of N_2 gas over a temperature range of 25 °C–250 °C.

Single crystal X-ray diffraction data.

Single crystal X-ray diffraction experiments were carried out using a Bruker D8 QUEST X-ray single crystal diffractometer. For the data collection, *omega* and *phi* scans were employed. The frames were integrated with the Bruker SAINT software package using a narrow-frame algorithm. The single crystal X-ray data were corrected for absorption effects using the Multi-Scan method (SADABS).

The structures were determined using direct methods and refined using (based on F^2 using all independent data (SHELXTL 97)) using the Bruker SHELXTL[1,2] Software Package. All non-hydrogen atoms were located from different Fourier maps and refined with anisotropic displacement parameters. Hydrogen atoms were added in riding positions.

Synthesis of ligand (1R,2R)-N,N'-bis(pyridine-3-ylmethil)cyclohexane-1,2-diamine (L)

(1*R*, 2*R*)-1, 2-diaminocyclohexane (2.54 g, 21 mmol) was dissolved in 30 ml methanol, and 3-pyridinecarboxaldehyde (4.50 g, 42 mmol) was slowly added. The reaction mixture was stirred for 6h at 60℃, and then cooled down to room temperature. Sodium

borohydride was added (1.8 g, 47.6 mmol) to the solution. Following a further 12h reaction time, the solvent was removed by rotary evaporation and 20 mL water was added to quench the excess sodium borohydride. The aqueous phase was extracted with DCM (3 ×15 ml) then combined methylene chloride layer was washed with water (2×20 mL). The separated organics were dried over sodium sulfate, filtered and the solvent evaporated to give the product **L** (5.84 g, 92.9 %).[3]

Synthesis of $[H_4L]^{4+}\cdot 4Cl^{-}\cdot(H_2O)$ (1)

30 mg (0.10 mmol) of **L** was dissolved by 5mL methanol and 5mL acetonitrile then 0.05mL concentrated hydrochloric acid was added. The flask was allowed to stand to evaporate for one week at r. t., giving rise to colorless transparent crystals **1**, m.p. 234.5-235.6 °C.

Synthesis of $[H_4L]^{4+}\cdot[CuCl_4]^{2-}\cdot 2Cl^{-}$ (2)

46 mg (0.1 mmol) of protonated **L** was dissolved by methanol and ethanol mixed solvents (10 mL，1:1) in a 25 mL Erlenmeyer flask, and then concentrated HCl (0.1 mL) and $CuCl_2\cdot 2H_2O$ (17 mg, 0.10 mmol) were added slowly to the flask, which was shaken until the contents has dissolved and allowing the solvents to slowly evaporate. Crystals grew in 3 days, giving rise to yellow needle crystals **2**, m.p. 169.8-171.2 °C.

Synthesis of $[H_4L]^{4+}\cdot[CuCl_3(H_2O)]^{-}\cdot 3Cl^{-}$ (3)

46 mg (0.10 mmol) of protonated **L** was dissolved by methanol (10 mL) in a 25 mL Erlenmeyer flask, and then concentrated HCl (0.10 mL) and $CuCl_2\cdot 2H_2O$ (17 mg, 0.10 mmol) were added slowly to the flask, which was shaken until the contents has dissolved，and allowing the solvents to slowly evaporate. Crystals grew in 10 days, giving rise to green needle crystals **3**. m.p. 168.7-170.1 °C.

Mechanochemical synthesis of $[H_4L]^{4+}\cdot[CuCl_3(H_2O)]^{-}\cdot 3Cl^{-}$ (3)

$CuCl_2\cdot 2H_2O$ (17 mg, 0.10 mmol) and 46 mg (0.10 mmol) of protonated **L** were ground

together for 5 min in an agate mortar with a drop of concentrated HCl. The resulting powder material was dried at 40 °C to remove any traces of water.

Dehydrochlorination reaction (3→4). Synthesis of [$LCuCl_2$] (4)

Salt **3** (58 mg, 0.10 mmol) and KOH (22.6 mg, 0.40 mmol) were ground together for 8 min in an agate mortar with a drop of methanol. The resulting light blue powder was dried under vacuum for a few minutes. The powder was dissolved by methanol and acetonitrile mixed solvents, 2 days later, giving rise to blue crystal **4**, m.p. 193.2-194.1 °C.

Chemisorption of HCl and H_2O Vapours. First-to-second coordination sphere reaction 4→3.

Micro-crystalline complex **4** (43 mg, 0.10 mmol) was placed in a vial inside a sealed jar containing concentrated HCl. The blue powder became green in 48 h.

Flux synthesis of complex 4

(1*R*, 2*R*)-*N*, *N*′-bis(pyridin-3-ylmethyl)cyclohexane-1,2-diamine (**L**) (59.6 mg, 0.2 mmol) and $CuCl_2 \cdot 2H_2O$ (34 mg, 0.2 mmol) were dissolved in 20 mL and 8 mL methanol, respectively. Then, the solution of $CuCl_2 \cdot 2H_2O$ was slowly added. The reaction mixture was stirred for one hour at 60℃, then cooled down to room temperature, and obtained blue precipitate of complex **4**.

Low-Pressure Nitrogen Adsorption/Desorption Measurements

Low pressure gas adsorption/desorption studies were conducted on a automated volumetric adsorption analyzers ASIQ-C (Quantachrome Instruments) at relative pressures up to 1 atm. The cryogenic temperature was controlled using liquid nitrogen baths at 77 K. The apparent surface areas were determined from the nitrogen adsorption/desorption isotherms collected at 77 K by applying the Brunauer-Emmett-Teller (BET).

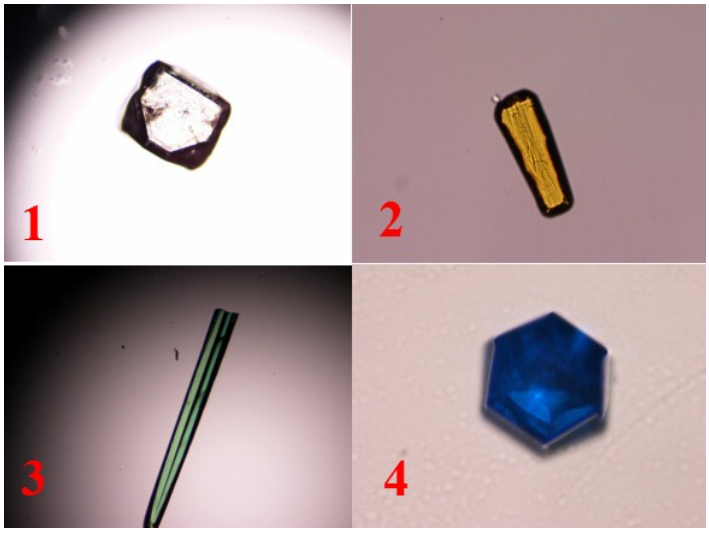

Figure S1. Images of the single crystals of compounds 1, **2**, **3**, and **4**.

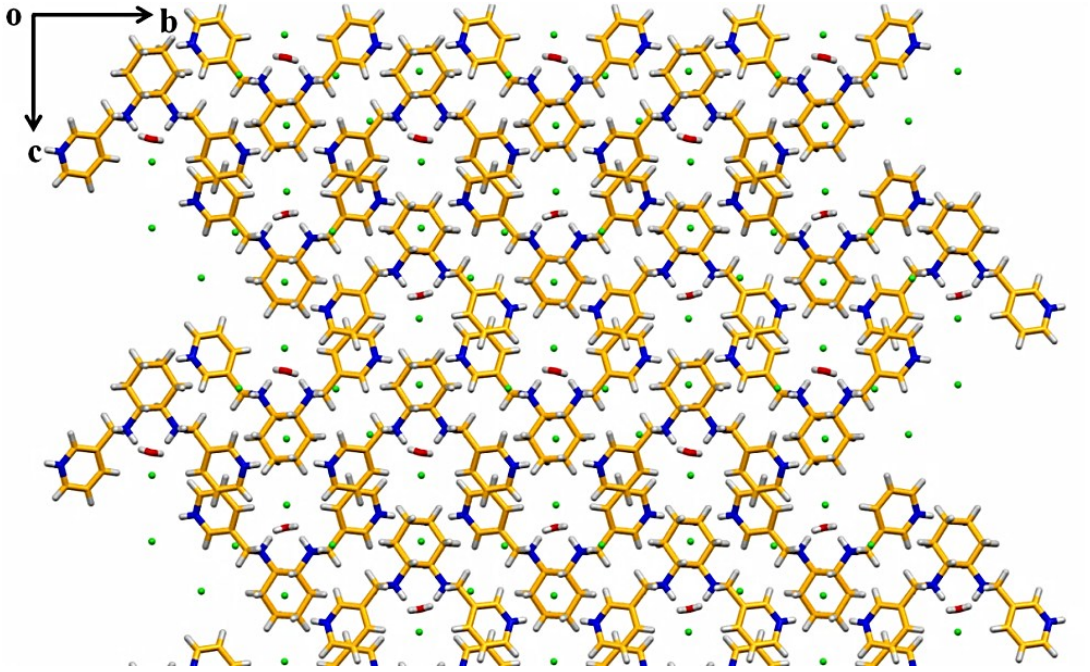

Figure S2. Packing of **1** viewed along the *a*-axis. Color code: carbon: orange; nitrogen: blue; oxygen: red; chloride: green; hydrogen: white.

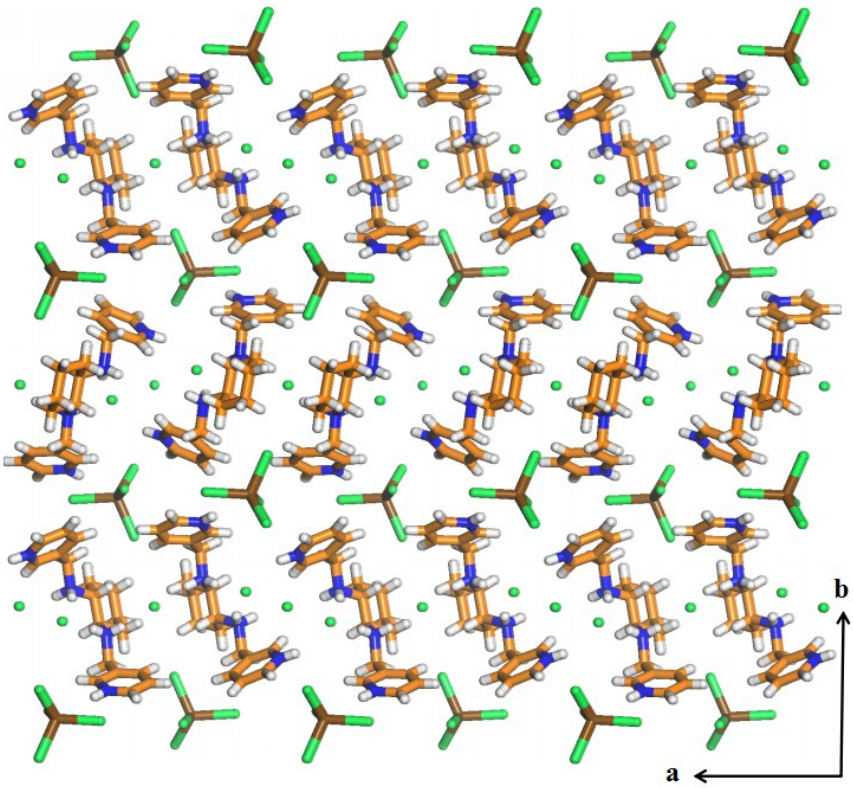

Figure S3. Packing of **2** viewed along the *c*-axis. Color code: carbon: orange; nitrogen: blue; chloride: green; copper: brown; hydrogen: white.

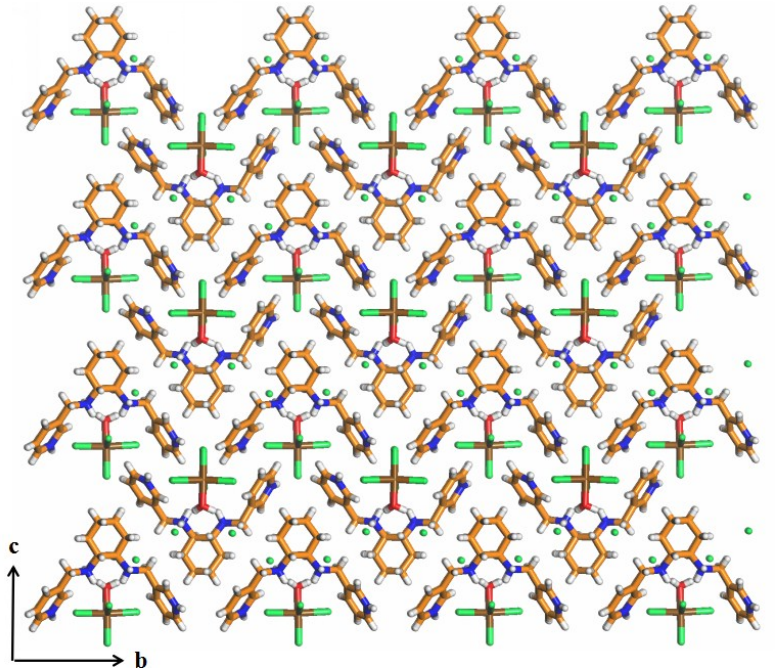

Figure S4. Packing of **3** viewed along the *a*-axis. Color code: carbon: orange; nitrogen: blue; oxygen**:** red**;** chloride: green; copper: brown; hydrogen: white.

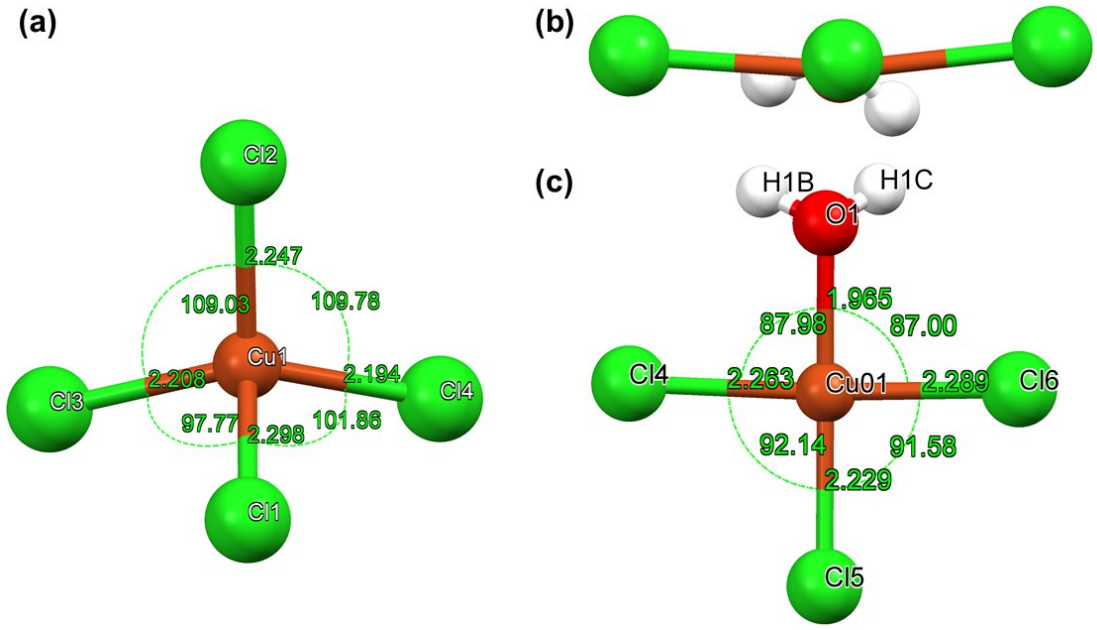

Figure S5. Coordination geometries around the $[CuCl_4]^{2-}$ metal center in **2** (a). The disordered atoms in the $[CuCl_4]^{2-}$ have not been shown for clarity purposes. View of the $[CuCl_3(H_2O)]^-$ in **3**: top (b) and side views (c).

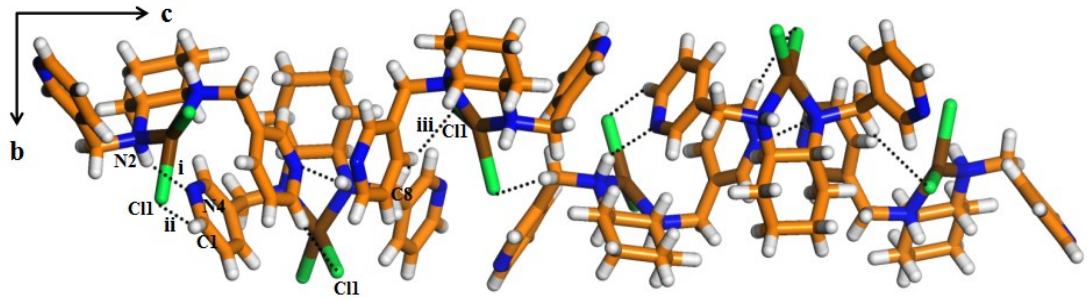

Figure S6. Crystal structure of **4** showing the hydrogen bond and short contacts along the *a*-axis. Color code: carbon: orange; nitrogen: blue; oxygen**:** red**;** chloride: green; copper: brown; hydrogen: white.

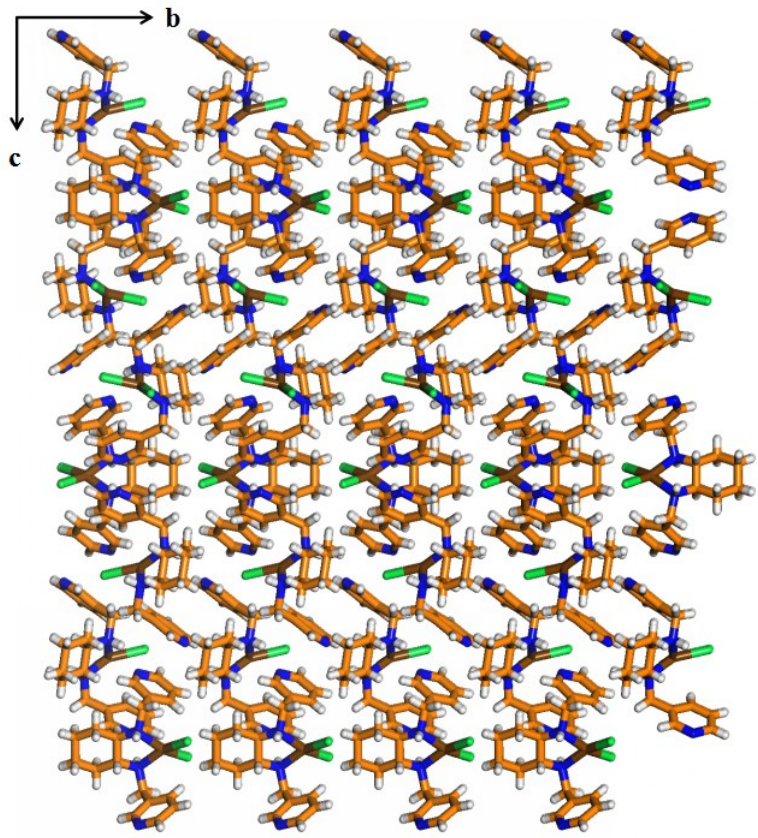

Figure S7. Packing of **4** viewed along the *a*-axis. Color code: carbon: orange; nitrogen: blue; oxygen**:** red**;** chloride: green; copper: brown; hydrogen: white.

Table S1. Hydrogen bonds in crystal **2**.

	D-H(Å)	D···A(Å)	H···A(Å)	D-H···A(°)	Symmetry Code
i	0.890(2)	3.110(2)	2.224(6)	173.12(6)	x, y, z
ii	0.890(4)	3.083(7)	2.230(7)	160.31(1)	x, y, z
iii	0.860(4)	3.223(2)	2.504(1)	141.63(2)	x, y, z
iv	0.890(6)	3.050(6)	2.165(9)	172.15(6)	x, y, z-1
v	0.890(2)	3.045(4)	2.161(3)	172.02(5)	x, y, z

Table S2. Hydrogen bonds in crystal **3**.

	D-H(Å)	D···A(Å)	H···A(Å)	D-H···A(°)	Symmetry Code
i	0.889(9)	3.142(4)	2.323(1)	153.06(3)	x, y, z
ii	0.890(6)	3.156(3)	2.272(8)	171.44(0)	x, y, z
iii	0.859(9)	3.330(7)	2.694(9)	131.84(4)	x, y, z
iv	0.890(3)	3.057(2)	2.173(7)	171.57(9)	x, y, z
v	0.890(4)	3.113(0)	2.249(5)	163.36(2)	x-1, y, z
vi	0.870(3)	3.542(3)	2.295(9)	148.51(4)	x, y, z
vii	0.870(2)	3.062(8)	2.262(6)	152.84(2)	x, y, z

Table S3. Hydrogen bond and short interactions in crystal **4**.

	D-H(Å)	D···A(Å)	H···A(Å)	D-H···A(°)	Symmetry Code
i	0.979(6)	3.202(1)	2.311(4)	150.74(3)	x-y, y, z+1/6
ii	0.929(5)	3.781(3)	2.944(7)	150.47(7)	y, -x+y, z-1/6
iii	0.969(2)	3.890(2)	2.945(9)	165.00(8)	x-y, -y-1, -z-1

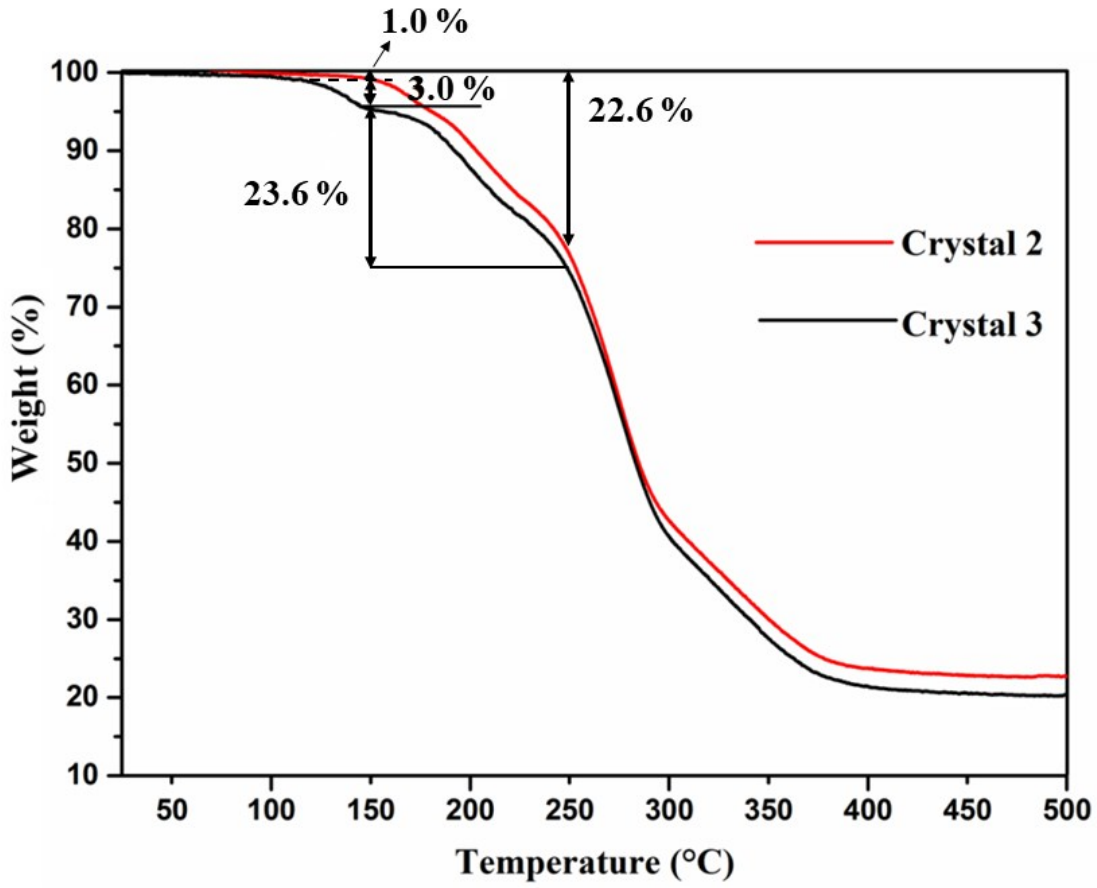

Figure S8. TGA plot showing the weight loss in **2** and **3**.

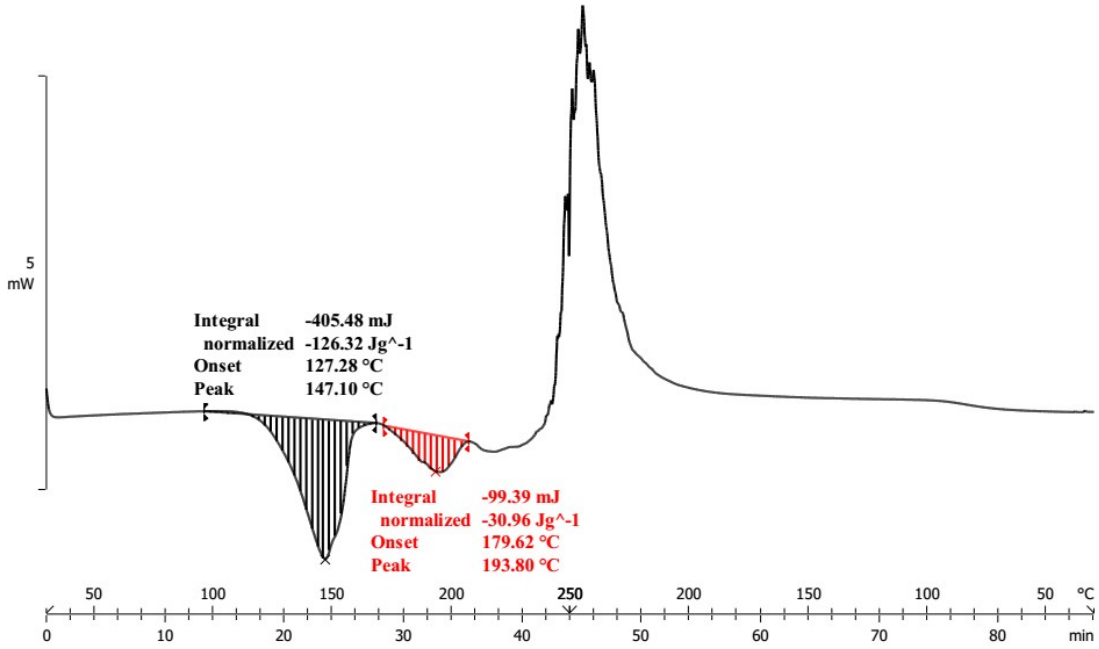

Figure S9. DSC corresponding to second sphere adduct **3**.

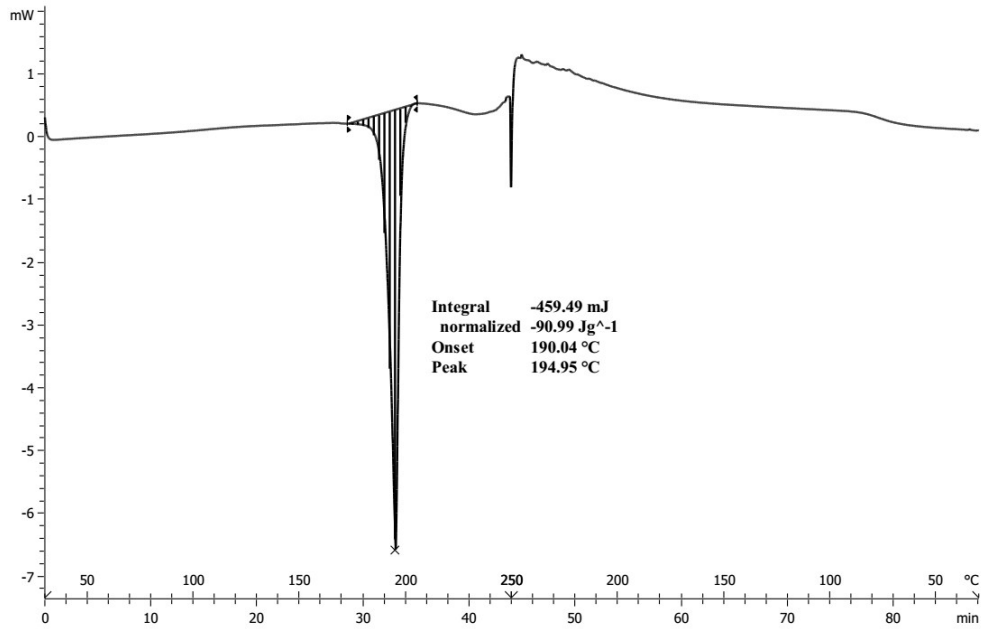

Figure S10. DSC corresponding to the coordination complex **4**.

Table S4. Low pressure nitrogen adsorption data summary for samples **3** and **4**.

Sample	**BET (m^2g^{-1})**	**P.V. (cm^3g^{-1})**
3	7.614	0.012
4	11.250	0.015

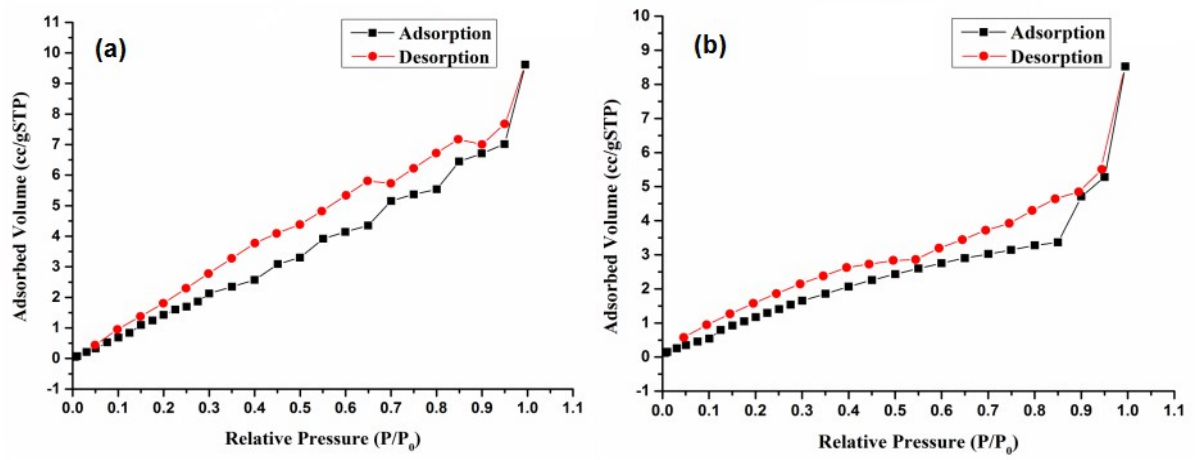

Figure S11. Nitrogen adsorption/desorption isotherms of the powder of **3** (a) and **4** (b).

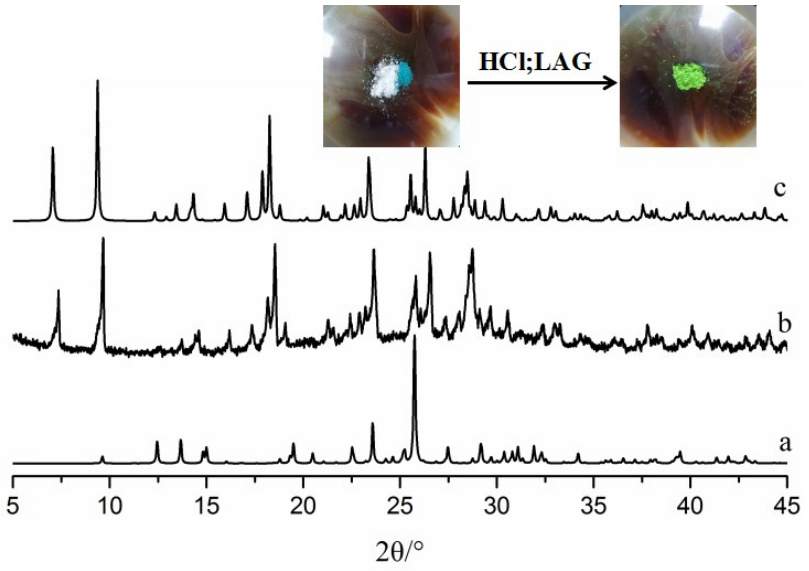

Figure S12. (a) Simulated XRPD from single crystal **1**. (b) The product of grinding salt of **L** and $CuCl_2 \cdot 2H_2O$ in 1:1 ratio with a drop of concentrated HCl and a drop of methanol for 5 minutes. (c) Simulated XRPD from single crystal **3**.

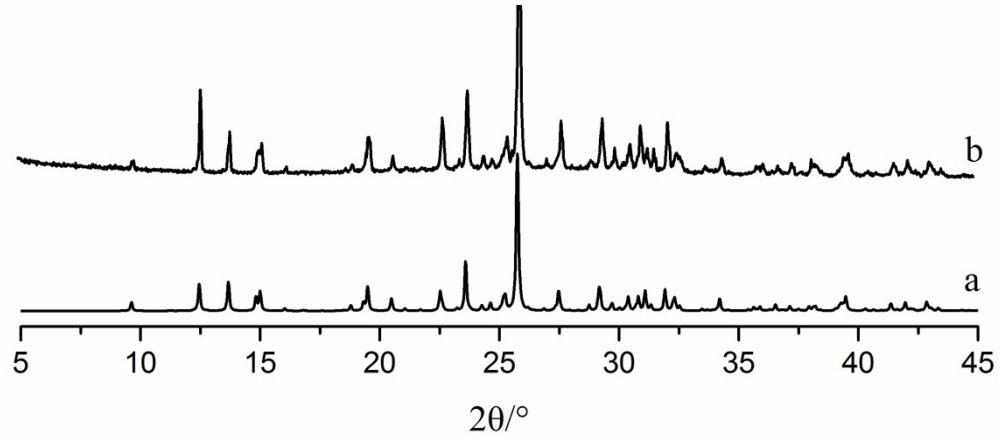

Figure S13. Experimental XRPD patterns of **1**: (a) Simulated XRPD from single crystal **1**; (b) Experimental XRPD from single crystal **1**.

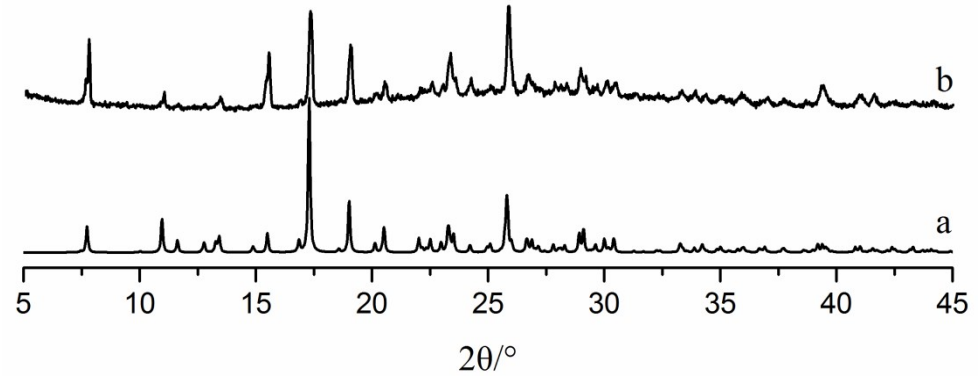

Figure S14. Experimental XRPD patterns of crystal **2**: (a) Simulated XRPD from single crystal **2**; (b) Experimental XRPD from single crystal **2**.

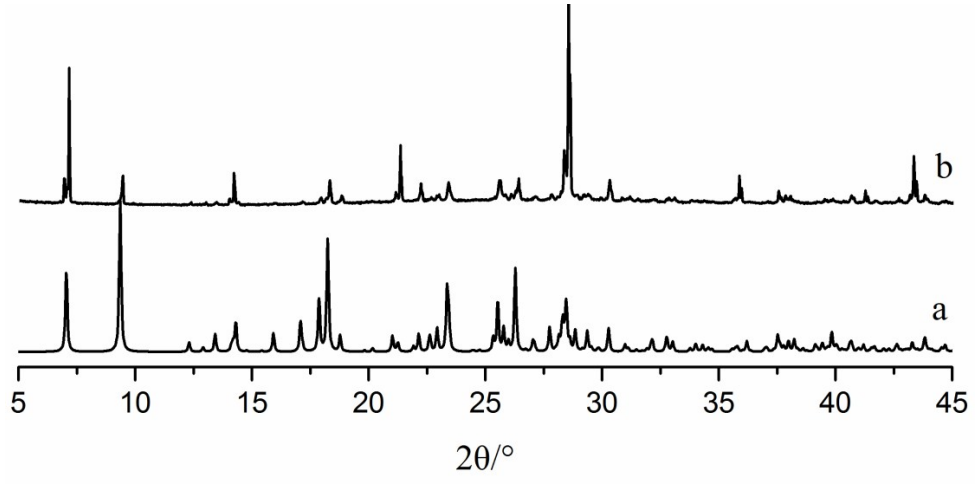

Figure S15. Experimental XRPD patterns of crystal **3**: (a) Simulated XRPD from single crystal **3**; (b) Experimental XRPD from single crystal **3**.

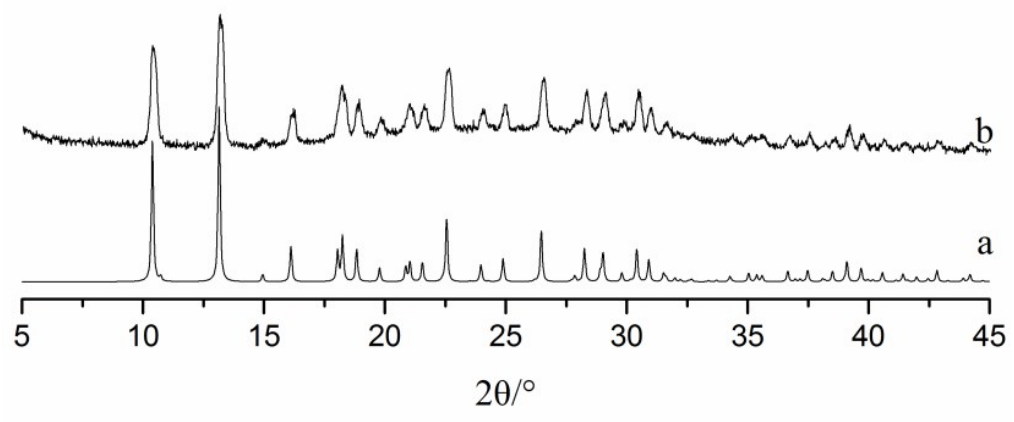

Figure S16. Experimental XRPD patterns of crystal **4**: (a) Simulated XRPD from single crystal **4**; (b) Experimental XRPD from single crystal **4**.

Table S5. Crystal data and structural refinement parameters for **1–4**.

	1	**2**	**3**	**4**
Empirical formula	C_{18} $H_{30}Cl_4N_4O$	$C_{18}H_{28}Cl_6CuN_4$	$C_{18}H_{30}Cl_6CuN_4O$	$C_{18}H_{24}Cl_2CuN_4$
Formula weight	460.26	574.67	594.71	430.85
Crystal temperature (K)	298	150(2)	298	298
Crystal system	Orthorhombic	Orthorhombic	Monoclinic	Hexagonal
Space group	$P2_12_12_1$	$P2_12_12$	$P2_1$	$P6_122$
Z	4	4	2	6
a(Å)	7.7024(11)	13.7107(8)	6.9923(5)	9.8247(4)
b(Å)	15.716(2)	23.0021(14)	14.3694(10)	9.8247(4)
c(Å)	18.368(3)	7.9717(4)	12.7878(9)	32.973(2)
α(deg)	90	90	90	90
β(deg)	90	90	101.514(2)	90
γ(deg)	90	90	90	120
V(Å^3)	2223.4(5)	2514.1(2)	1259.00(15)	2756.3(3)
D_x(Mg.cm^{-3})	1.375	1.518	1.569	1.558
μ(mm^{-1})	0.548	1.519	1.523	1.488
F(000)	968	1172	610	1338
R_{int}	0.0247	0.0357	0.0247	0.0395
No.of collected data(unique)	28774	11177	21527	51693
No.of data with I>2σ(I)	5401	4428	6090	2269
No.of parameters varied	252	287	272	115
s	1.120	1.044	1.074	1.174
R_f/wR_f	0.0323/0.0789	0.0650/0.1568	0.0368/0.0979	0.0322/0.0789
All data R_f/wR_f	0.0342/0.0775	0.0867/0.1691	0.0377/0.0973	0.0333/0.0783

Molecular Modelling Data

Solid-state density functional theory (DFT) calculations were performed by employing the GGA PBE functional.[4] Double zeta numerical basis sets centered on atoms have been used. In particular, double basis set with polarisation functions on heavy atoms (i.e. DND set roughly comparable with 6-31G* gaussian contracted basis) and with polarisation functions on all atoms (i.e. DNP set roughly comparable with 6-31G** gaussian contracted basis). A Pseudopotential set of parameters has been used for Cu atoms.[25] Explicit van der Waals corrections[6] were also included as these terms can be important for subtle inter and intra-particle interactions.[7] The efficient numerical algorithms implemented into DMol^3 package[8] were employed in all the calculations.

Fixed experimental X-ray determined unit cells were used while atomic coordinates of all atoms are free to relax assuming space group constraints. The sublimation energies have been estimated as the difference (normalised by the

number of the complex particles) between the unit cell energy and the sum of the energy of the free particles and the energy of the rest of the crystalline cell.

Table S6 DFT energies relating to the reaction $[CuCl_4]^{2-} + H_2O \rightarrow [CuCl_3H_2O]^- + Cl^-$. Total energies are reported in hartree while differences both in hartree and kcal/mol.

Method	**$[CuCl_4]^{2-}$**	**H_2O**	**$[CuCl_3H_2O]^-$**	**Cl^-**	**ΔE(hartree)**	**kcal/mol**
PBE/DND	-2037.730423	-76.3631697	-1654.090763	-460.0675047	-0.06467	-40.58
PBE/DNP	-2037.751916	-76.3763813	-1654.110916	-460.0845112	-0.06713	-42.12

Table S7 Solid state DFT energies relating to crystalline structures **2** and **3**. Total energies are reported in hartree while differences both in hartree and kcal/mol.

Method	**2**	**2-$[CuCl_4]^{2-}$**	**$[CuCl_4]^{2-}$**	**ΔE(hartree)**	**kcal/mol**
PBE/DND	-15515.63197	-7363.010011	-2037.730423	-0.42507	-266.733
PBE/DNP	-15515.93645	-7363.342621	-2037.751916	-0.39654	-248.833

Method	**3**	**3-CuCl3H20**	**$[CuCl_3H_2O]^-$**	**ΔE(hartree)**	**kcal/mol**
PBE/DND	-7910.606574	-4601.912687	-1654.090763	-0.25618	-160.756
PBE/DNP	-7910.775216	-4602.093054	-1654.110916	-0.23017	-144.431

Geometrical parameters of structures 2 and 3 optimised at the PBE/DNP level are listed in pdb format.

Structure 2

```
REMARK    2 PDB file
REMARK    Created:  Sat Apr 06 17:55:07 ora solare Europa occidentale 2019
CRYST1   13.850   22.857    8.068  90.00  90.00  90.00 P21212
ORIGX1      1.000000    0.000000    0.000000        0.00000
ORIGX2      0.000000    1.000000    0.000000        0.00000
ORIGX3      0.000000    0.000000    1.000000        0.00000
SCALE1      0.072205    0.000000    0.000000        0.00000
SCALE2      0.000000    0.043750    0.000000        0.00000
SCALE3      0.000000    0.000000    0.123954        0.00000
ATOM      1 Cu1  MOL     2       4.876    5.813    8.027  1.00  0.06          Cu2+
ATOM      2 Cl1  MOL     2       5.294    5.121    5.831  0.70  0.09          Cl1-
ATOM      3 Cl2  MOL     2       2.580    6.070    8.257  1.00  0.07          Cl1-
ATOM      4 Cl3  MOL     2       5.749    7.917    8.061  1.00  0.08          Cl1-
ATOM      5 Cl4  MOL     2       5.622    4.295    9.531  0.70  0.19          Cl1-
ATOM      6 Cl7  MOL     2       4.636    0.858    3.543  1.00  0.06          Cl1-
ATOM      7  N1  MOL     2       4.328   -0.782    0.896  1.00  0.06           N1+
ATOM      8  H1A MOL     2       4.323   -0.292    1.833  1.00  0.07           H
ATOM      9  H1B MOL     2       5.211   -0.427    0.397  1.00  0.07           H
ATOM     10  N2  MOL     2       2.430    1.563    1.428  1.00  0.04           N1+
ATOM     11  H2A MOL     2       3.207    1.398    2.128  1.00  0.05           H
ATOM     12  H2B MOL     2       1.591    0.995    1.772  1.00  0.05           H
ATOM     13  N3  MOL     2       2.453    4.476    4.901  1.00  0.08           N
ATOM     14  H3  MOL     2       3.278    4.815    5.468  1.00  0.09           H
ATOM     15  N4  MOL     2       6.596   -2.444    4.196  1.00  0.09           N
ATOM     16  H4  MOL     2       7.538   -2.062    4.444  1.00  0.11           H
ATOM     17  C1  MOL     2       3.115   -0.437    0.058  1.00  0.04           C
```

ATOM	18	H1	MOL	2	2.262	-0.961	0.523	1.00	0.05	H
ATOM	19	C2	MOL	2	2.814	1.073	0.043	1.00	0.04	C
ATOM	20	H2	MOL	2	3.710	1.647	-0.258	1.00	0.05	H
ATOM	21	C3	MOL	2	2.075	3.024	1.474	1.00	0.05	C
ATOM	22	H3A	MOL	2	2.929	3.583	1.072	1.00	0.07	H
ATOM	23	H3B	MOL	2	1.200	3.187	0.837	1.00	0.07	H
ATOM	24	C4	MOL	2	1.748	3.497	2.862	1.00	0.05	C
ATOM	25	C5	MOL	2	2.757	3.985	3.684	1.00	0.07	C
ATOM	26	H5	MOL	2	3.809	4.017	3.388	1.00	0.08	H
ATOM	27	C6	MOL	2	1.194	4.543	5.383	1.00	0.08	C
ATOM	28	H6	MOL	2	1.073	4.995	6.370	1.00	0.09	H
ATOM	29	C7	MOL	2	0.151	4.064	4.604	1.00	0.10	C
ATOM	30	H7	MOL	2	-0.865	4.129	4.993	1.00	0.12	H
ATOM	31	C8	MOL	2	0.428	3.537	3.340	1.00	0.07	C
ATOM	32	H8	MOL	2	-0.379	3.182	2.696	1.00	0.09	H
ATOM	33	C9	MOL	2	1.641	1.350	-0.914	1.00	0.05	C
ATOM	34	H9A	MOL	2	1.479	2.433	-0.986	1.00	0.07	H
ATOM	35	H9B	MOL	2	0.725	0.926	-0.465	1.00	0.07	H
ATOM	36	C10	MOL	2	1.848	0.787	-2.316	1.00	0.06	C
ATOM	37	AH10	MOL	2	0.947	0.978	-2.920	1.00	0.07	H
ATOM	38	BH10	MOL	2	2.682	1.309	-2.816	1.00	0.07	H
ATOM	39	C11	MOL	2	2.155	-0.705	-2.281	1.00	0.05	C
ATOM	40	AH11	MOL	2	2.389	-1.064	-3.296	1.00	0.06	H
ATOM	41	BH11	MOL	2	1.280	-1.279	-1.929	1.00	0.06	H
ATOM	42	C12	MOL	2	3.341	-0.981	-1.361	1.00	0.05	C
ATOM	43	AH12	MOL	2	3.506	-2.067	-1.293	1.00	0.06	H
ATOM	44	BH12	MOL	2	4.255	-0.526	-1.785	1.00	0.06	H
ATOM	45	C13	MOL	2	4.476	-2.273	1.117	1.00	0.10	C
ATOM	46	AH13	MOL	2	3.503	-2.744	0.923	1.00	0.12	H
ATOM	47	BH13	MOL	2	5.190	-2.657	0.377	1.00	0.12	H

```
ATOM     48  C14 MOL     2       4.943  -2.604   2.505  1.00  0.05           C
ATOM     49  C15 MOL     2       6.178  -2.147   2.955  1.00  0.07           C
ATOM     50  H15 MOL     2       6.874  -1.553   2.361  1.00  0.08           H
ATOM     51  C16 MOL     2       5.883  -3.195   5.062  1.00  0.11           C
ATOM     52  H16 MOL     2       6.335  -3.389   6.035  1.00  0.14           H
ATOM     53  C17 MOL     2       4.657  -3.701   4.656  1.00  0.10           C
ATOM     54  H17 MOL     2       4.095  -4.325   5.355  1.00  0.12           H
ATOM     55  C18 MOL     2       4.182  -3.394   3.374  1.00  0.09           C
ATOM     56  H18 MOL     2       3.218  -3.790   3.038  1.00  0.11           H
ATOM     57 Cl5  MOL     2       6.925   0.000   7.533  1.00  0.24          Cl1-
ATOM     58 Cl6  MOL     2       0.000   0.000   2.455  1.00  0.07          Cl1-
TER      59
CONECT    2    3    4    5    6
CONECT    3    2
CONECT    4    2
CONECT    5    2
CONECT    6    2
CONECT    8    9   10   18   46
CONECT    9    8
CONECT   10    8
CONECT   11   12   13   20   22
CONECT   12   11
CONECT   13   11
CONECT   14   15   26   28
CONECT   15   14
CONECT   16   17   50   52
CONECT   17   16
CONECT   18    8   19   20   43
CONECT   19   18
CONECT   20   11   18   21   34
```

CONECT 21 20

CONECT 22 11 23 24 25

CONECT 23 22

CONECT 24 22

CONECT 25 22 26 32

CONECT 26 14 25 27

CONECT 27 26

CONECT 28 14 29 30

CONECT 29 28

CONECT 30 28 31 32

CONECT 31 30

CONECT 32 25 30 33

CONECT 33 32

CONECT 34 20 35 36 37

CONECT 35 34

CONECT 36 34

CONECT 37 34 38 39 40

CONECT 38 37

CONECT 39 37

CONECT 40 37 41 42 43

CONECT 41 40

CONECT 42 40

CONECT 43 18 40 44 45

CONECT 44 43

CONECT 45 43

CONECT 46 8 47 48 49

CONECT 47 46

CONECT 48 46

CONECT 49 46 50 56

CONECT 50 16 49 51

CONECT 51 50

CONECT 52 16 53 54

CONECT 53 52

CONECT 54 52 55 56

CONECT 55 54

CONECT 56 49 54 57

CONECT 57 56

END

Structure 3

REMARK 3 PDB file

REMARK Created: Sat Apr 06 17:54:28 ora solare Europa occidentale 2019

CRYST1 6.992 14.369 12.788 90.00 101.51 90.00 P21

ORIGX1 1.000000 0.000000 0.000000 0.00000

ORIGX2 0.000000 1.000000 0.000000 0.00000

ORIGX3 0.000000 0.000000 1.000000 0.00000

SCALE1 0.143014 0.000000 0.029133 0.00000

SCALE2 0.000000 0.069592 0.000000 0.00000

SCALE3 0.000000 0.000000 0.079806 0.00000

ATOM 1 Cu01 MOL 2 4.711 7.229 11.262 1.00 0.03 Cu2+

ATOM 2 Cl3 MOL 2 3.941 5.178 7.298 1.00 0.04 Cl1-

ATOM 3 Cl6 MOL 2 4.717 4.946 11.160 1.00 0.04 Cl1-

ATOM 4 Cl2 MOL 2 1.631 7.410 10.607 1.00 0.04 Cl1-

ATOM 5 Cl5 MOL 2 4.715 7.119 13.573 1.00 0.04 Cl1-

ATOM 6 Cl4 MOL 2 4.927 9.498 11.309 1.00 0.04 Cl1-

ATOM 7 Cl1 MOL 2 4.737 9.494 7.230 1.00 0.05 Cl1-

ATOM 8 O1 MOL 2 5.076 7.242 9.255 1.00 0.03 O

ATOM 9 H1B MOL 2 4.773 8.075 8.782 1.00 0.05 H

ATOM 10 H1C MOL 2 4.614 6.495 8.765 1.00 0.05 H

ATOM	11	N4	MOL	2	1.018	5.755	8.067	1.00	0.02	N1+
ATOM	12	H4A	MOL	2	2.053	5.565	7.875	1.00	0.03	H
ATOM	13	H4B	MOL	2	0.993	6.276	8.993	1.00	0.03	H
ATOM	14	N3	MOL	2	0.700	8.871	8.030	1.00	0.02	N1+
ATOM	15	H3A	MOL	2	-0.341	8.990	7.860	1.00	0.03	H
ATOM	16	H3B	MOL	2	0.856	8.414	8.977	1.00	0.03	H
ATOM	17	N1	MOL	2	2.114	2.958	11.129	1.00	0.03	N
ATOM	18	H1	MOL	2	3.024	3.060	11.628	1.00	0.04	H
ATOM	19	C7	MOL	2	0.539	6.626	6.915	1.00	0.02	C
ATOM	20	H7	MOL	2	-0.540	6.789	7.063	1.00	0.03	H
ATOM	21	C14	MOL	2	0.965	10.992	9.341	1.00	0.02	C
ATOM	22	C12	MOL	2	1.281	7.985	6.937	1.00	0.02	C
ATOM	23	H12	MOL	2	2.342	7.831	7.202	1.00	0.03	H
ATOM	24	C4	MOL	2	0.644	3.652	9.402	1.00	0.02	C
ATOM	25	C5	MOL	2	1.870	3.735	10.051	1.00	0.03	C
ATOM	26	H5	MOL	2	2.691	4.395	9.766	1.00	0.03	H
ATOM	27	C15	MOL	2	1.886	11.055	10.398	1.00	0.04	C
ATOM	28	H15	MOL	2	2.834	10.509	10.336	1.00	0.05	H
ATOM	29	C8	MOL	2	0.775	5.831	5.622	1.00	0.04	C
ATOM	30	H8A	MOL	2	1.801	5.428	5.652	1.00	0.05	H
ATOM	31	H8B	MOL	2	0.089	4.972	5.597	1.00	0.05	H
ATOM	32	C13	MOL	2	1.307	10.250	8.077	1.00	0.03	C
ATOM	33	AH13	MOL	2	0.942	10.804	7.200	1.00	0.04	H
ATOM	34	BH13	MOL	2	2.398	10.127	7.998	1.00	0.04	H
ATOM	35	C1	MOL	2	1.222	2.084	11.636	1.00	0.04	C
ATOM	36	H1A	MOL	2	1.510	1.545	12.540	1.00	0.05	H
ATOM	37	C16	MOL	2	1.606	11.809	11.538	1.00	0.04	C
ATOM	38	H16	MOL	2	2.331	11.883	12.353	1.00	0.05	H
ATOM	39	C18	MOL	2	-0.240	11.680	9.479	1.00	0.04	C
ATOM	40	H18	MOL	2	-1.025	11.655	8.723	1.00	0.05	H

```
ATOM     41   C3  MOL     2      -0.299    2.735    9.902  1.00  0.04           C
ATOM     42   H3  MOL     2      -1.274    2.650    9.416  1.00  0.05           H
ATOM     43   C6  MOL     2       0.286    4.458    8.188  1.00  0.03           C
ATOM     44  H6A MOL     2       0.483    3.855    7.287  1.00  0.04           H
ATOM     45  H6B MOL     2      -0.792    4.675    8.190  1.00  0.04           H
ATOM     46  C10 MOL     2       1.557    7.861    4.400  1.00  0.06           C
ATOM     47 AH10 MOL     2       1.464    8.453    3.477  1.00  0.07           H
ATOM     48 BH10 MOL     2       2.609    7.526    4.465  1.00  0.07           H
ATOM     49  C11 MOL     2       1.206    8.735    5.598  1.00  0.04           C
ATOM     50 AH11 MOL     2       1.893    9.592    5.638  1.00  0.05           H
ATOM     51 BH11 MOL     2       0.190    9.147    5.467  1.00  0.05           H
ATOM     52   C2  MOL     2      -0.010    1.954   11.018  1.00  0.05           C
ATOM     53   H2  MOL     2      -0.762    1.284   11.439  1.00  0.06           H
ATOM     54   N2  MOL     2      -0.480   12.393   10.599  1.00  0.08           N
ATOM     55  H2A MOL     2      -1.392   12.902   10.738  1.00  0.10           H
ATOM     56   C9  MOL     2       0.627    6.657    4.353  1.00  0.05           C
ATOM     57  H9A MOL     2      -0.418    7.003    4.234  1.00  0.06           H
ATOM     58  H9B MOL     2       0.858    6.023    3.483  1.00  0.06           H
ATOM     59  C17 MOL     2       0.400   12.484   11.619  1.00  0.07           C
ATOM     60  H17 MOL     2       0.103   13.101   12.474  1.00  0.08           H
TER      61
CONECT    1   60
CONECT    2    4    6    7    9
CONECT    4    2
CONECT    6    2
CONECT    7    2
CONECT    9    2   10   11
CONECT   10    9
CONECT   11    9
CONECT   12   13   14   20   44
```

CONECT 13 12

CONECT 14 12

CONECT 15 16 17 23 33

CONECT 16 15

CONECT 17 15

CONECT 18 19 26 36

CONECT 19 18

CONECT 20 12 21 23 30

CONECT 21 20

CONECT 22 28 33 40

CONECT 23 15 20 24 50

CONECT 24 23

CONECT 25 26 42 44

CONECT 26 18 25 27

CONECT 27 26

CONECT 28 22 29 38

CONECT 29 28

CONECT 30 20 31 32 57

CONECT 31 30

CONECT 32 30

CONECT 33 15 22 34 35

CONECT 34 33

CONECT 35 33

CONECT 36 18 37 53

CONECT 37 36

CONECT 38 28 39 60

CONECT 39 38

CONECT 40 22 41 55

CONECT 41 40

CONECT 42 25 43 53

CONECT 43 42

CONECT 44 12 25 45 46

CONECT 45 44

CONECT 46 44

CONECT 47 48 49 50 57

CONECT 48 47

CONECT 49 47

CONECT 50 23 47 51 52

CONECT 51 50

CONECT 52 50

CONECT 53 36 42 54

CONECT 54 53

CONECT 55 40 56 60

CONECT 56 55

CONECT 57 30 47 58 59

CONECT 58 57

CONECT 59 57

CONECT 60 38 55 1

END

References

1 Sheldrick, G. M. *SHELXTL Reference Manual* (Siemens Analytical X-ray Systems, Inc., Madison, Wisconsin, USA), **1996.**

2 Sheldrick, G. M. *Acta Cryst.* **2008**, *A64*, 112–122.

3 Cooper, C. J.; Jones, M. D.; Brayshaw, S. K.; Sonnex, B.; Russell, M. L.; Mahon M. F.; Allan, D. R. When is an imine not an imine? Unusual reactivity of a series of Cu(II) imine-pyridine complexes and their exploitation for the Henry reaction. *Dalton Trans.* **2011**, *40*, 3677–3682.

4 (a) Perdew, J. P.; Burke K.; Ernzerhof, M. E. Generalized Gradient

Approximation Made Simple. *Phys. Rev. Lett.* **1996**, *77*, 3865–3868. (b) Perdew, J. P.; Burke K.; Ernzerhof, M. E. Generalized Gradient Approximation Made Simple. *Phys. Rev. Lett.* **1997**, *78*, 1396–1396.

5 (a) Dolg, M.; Wedig, U.; Stoll, H.; Preuss, H. Energy-adjusted ab initio pseudopotentials for the first row transition elements. *J. Chem. Phys.* 1987, 86, 866–872. (b) Bergner, A.; Dolg, M.; Küechle, W.; Stoll, H.; Preuss, H. Ab initio energy-adjusted pseudopotentials for elements of groups 13–17. *Mol. Phys.* **1993**, *80*, 1431–1441.

6 Grimme, S. Semiempirical hybrid density functional with perturbative second-order correlation. *J. Chem. Phys*. **2006**, *124*, 34108.

7 (a) Baggioli, A.; Meille, S. V.; Raos, G.; Po, R.; Brinkmann M.; Famulari, A. Intramolecular CH/π interactions in alkylaromatics: Monomer conformations for poly(3-alkylthiophene) atomistic models. *Int. J. Quantum Chem*. **2013**, *113*, 2154–2162. (b) Baggioli A.; Famulari, A. On the inter-ring torsion potential of regioregular P3HT: a first principles reexamination with explicit side chains. *Phys. Chem. Chem. Phys*. **2014**, *16*, 3983–3994.

8 Delley, B. From molecules to solids with the DMol^3 approach. *J. Chem. Phys.* **2000**, *113*, 7756–7764.